Journal of Hydrology (2008) 349, 489–500

available at www.sciencedirect.com

ScienceDirect

journal homepage: www.elsevier.com/locate/jhydrol

Continuous measurement of water vapor D/H and $^{18}O/^{16}O$ isotope ratios in the atmosphere

Xue-Fa Wen [a], Xiao-Min Sun [a], Shi-Chun Zhang [a], Gui-Rui Yu [a], Steve D. Sargent [b], Xuhui Lee [c,*]

[a] *Key Laboratory of Ecosystem Network Observation and Modeling, Institute of Geographic Sciences and Natural Resources Research, Chinese Academy of Sciences, Beijing, China*
[b] *Campbell Scientific, Inc., Logan, UT, USA*
[c] *School of Forestry and Environmental Studies, Yale University, New Haven, 21 Sachem St., New Haven, CT 06510, USA*

Received 16 March 2007; received in revised form 14 November 2007; accepted 19 November 2007

KEYWORDS
Stable isotopes;
Atmospheric water vapor;
Hydrogen isotope;
Oxygen isotope;
TDLAS

Summary The D/H and $^{18}O/^{16}O$ ratios in atmospheric water vapor provide rich information on the hydrological cycle and gaseous exchange processes between the terrestrial vegetation and the atmosphere. In this paper, we have demonstrated the feasibility to simultaneously measure both D/H and $^{18}O/^{16}O$ in atmospheric water vapor using a tunable diode laser absorption spectrometer. Our laboratory tests showed that the 1-h precision (one standard deviation) was 1.1‰ for D/H and 0.07‰ for $^{18}O/^{16}O$ at the dewpoint temperature of 15 °C. The difference between the laser measurement and cold trap/mass spectrometer analysis was 1.2 ± 6.0‰ (hourly mean ± one standard deviation) for D/H and 1.1 ± 1.3‰ for $^{18}O/^{16}O$. Our atmospheric measurement captured the rapidly changing isotopic signals in both D/H and $^{18}O/^{16}O$. The measured isotope ratios were highly correlated with the water vapor mixing ratio as expected and followed very closely the Global Meteoric Water Line except during two transitional periods when the deuterium excess of atmospheric vapor deviated from the standard value. In addition, we have refined a method to provide independent, timely performance test of the in situ system.

Introduction

The stable isotopes of water, HDO, $H_2{}^{18}O$, and $H_2{}^{16}O$, are powerful tracers for studies of the hydrologic cycle, ecological processes and paleoclimate (Jouzel et al., 1987; Gat et al., 2003; Ciais et al., 1995; Yakir and Sternberg, 2000; Vimeux et al., 2001; Kavanaugh and Cuffey, 2003; Peng et al., 2004). There is a growing interest in simultaneous measurement of the D/H and $^{18}O/^{16}O$ ratios of water in the environment. This is because HDO and $H_2{}^{18}O$ behave differently in the atmospheric water cycle. For example,

* Corresponding author. Tel.: +1 203 432 6271; fax: +1 203 432 5023.
E-mail address: xuhui.lee@yale.edu (X. Lee).

0022-1694/$ - see front matter © 2007 Elsevier B.V. All rights reserved.
doi:10.1016/j.jhydrol.2007.11.021

spatial and temporal variations of the two isotopes will result from the difference in the relative importance of the equilibrium and kinetic fractionation effects between HDO and $H_2{}^{18}O$ (Majoube, 1971; Merlivat, 1978; Horita and Wesolowski, 1994; Cappa et al., 2003). In the case of liquid/vapor equilibrium, the equilibrium fractionation effect of D/H is 8.3–9.6 times higher than that of $^{18}O/^{16}O$ in typical environmental temperature conditions (Majoube, 1971; Horita and Wesolowski, 1994). In comparison, the kinetic fractionation effect of D/H is 0.52 times lower than that of $^{18}O/^{16}O$ (Cappa et al., 2003). Quantification of both the D/H and $^{18}O/^{16}O$ ratios in the three phases of water has the potential of providing insights on the atmospheric water cycle that would otherwise be difficult by studying either the D/H or the $^{18}O/^{16}O$ ratio separately (Craig, 1961; Jouzel, 1986; Gat, 1996; Dawson et al., 1998; Cappa et al., 2003; Peng et al., 2004).

Since the development of stable isotope mass spectrometry, global and local patterns of the D/H and $^{18}O/^{16}O$ variations in precipitation have been extensively investigated (Craig, 1961; Dansgaard, 1964; Merlivat and Jouzel, 1979). The basic locus line for the liquid phase, $\delta D = 8\delta^{18}O + 10$, known as the Global Meteoric Water Line (GMWL), defines the isotopic relationship of continental precipitation that has not experienced evaporation (Craig, 1961; Jouzel, 1986; Gat, 1996). Here we use the usual delta notation such that $\delta = (R/R_{vsmow} - 1) \times 1000‰$, where R_{vsmow} = 0.00015576 for D/H and 0.0020052 for $^{18}O/^{16}O$, and R is the isotope molar ratio. The GMWL slope is determined by the ratio between the equilibrium fractionation effects of hydrogen and oxygen, while the intercept is controlled by the kinetic fractionation occurring during non-equilibrium processes such as evaporation (Craig, 1961; Jouzel et al., 2000; Cappa et al., 2003). Spatial and temporal variability of the isotope contents of precipitation depends on a host of atmospheric and geographic parameters such as temperature, precipitation amount, latitude, altitude, and distance to the coast (Dansgaard, 1964; Gat, 1980). These parameters also determine the different depletion in the isotopic ratios of local meteoric water lines compared to the GMWL. The intercept parameter, d ($=\delta D - 8\delta^{18}O$), termed deuterium excess, contains information on meteorological conditions at distant evaporative sources (Armengaud et al., 1998). The deuterium excess of precipitation provides information on the climatic conditions at the oceanic source region, but can be modified by vapor evaporated in continental basins (Araguás-Araguás et al., 2000). Direct measurement of d in the vapor phase may offer constraints on how to separate local evaporative contribution to the atmospheric water vapor (Gat, 1996; Araguás-Araguás et al., 2000).

To date, there are only a few studies that deal with both the D/H and $^{18}O/^{16}O$ ratios of atmospheric water vapor (Craig and Gordon, 1965; Brunel et al., 1992; Araguás-Araguás et al., 2000; Gat et al., 2003; Webster and Heymsfield, 2003; Franz and Rochmann, 2005; Worden et al., 2007). Because of technical and instrumental limitations, these studies are limited to discrete campaigns and discrete, point-in-time samples. Continuous and simultaneous measurement of HDO and $H_2{}^{18}O$ of atmospheric water vapor should provide an improved understanding of the mechanisms of evaporation and transpiration at the surface of the earth and the subsequent transport and phase changes in the atmosphere (Gat, 1996; He and Smith, 1999; Lee et al., 2006).

So far, several designs for the direct measurement of atmospheric vapor isotopic content have been reported in the literature (Griffith et al., 2006; Kerstel et al., 2006; Gupta et al., 2005; Lee et al., 2005; Webster and Heymsfield, 2003). Such measurement can provide new information on the gaseous exchange between the terrestrial vegetation and the atmosphere (Yakir and Sternberg, 2000; Lai et al., 2006). Several recent studies have demonstrated the feasibility of real-time observations of the isotopic gaseous exchange of $^{13}C-CO_2$ (Bowling et al., 2003; Griffis et al., 2004), $^{18}O-CO_2$ (Griffis et al., 2005) and $^{18}O-H_2O$ (Lee et al., 2007). Since the isotopic flux of these species is influenced by a similar set of biological and meteorological variables, simultaneous observations of multiple isotopes, as proposed in this study, will provide additional constraints on the hydrological and ecological processes of the ecosystem under investigation, such as flux partitioning (Yakir and Wang, 1996), leaf water enrichment (Lee et al., 2007), and canopy discrimination mechanisms (Lai et al., 2004).

An earlier paper reported the performance evaluation of a system for in situ measurement of the $^{18}O/^{16}O$ ratio in atmospheric water vapor (Lee et al., 2005). In this study, we configured the system to measure simultaneously the D/H and $^{18}O/^{16}O$ isotope ratios. Our first objective was to characterize the accuracy and precision of the measurement of these isotope ratios and determine the suitability of the system for long-term and uninterrupted operation. As discussed above, our work was motivated by the potential of such simultaneous measurement for hydrological and ecological applications. A detailed characterization of system performance is a necessary step before such applications can be achieved.

Our second objective was to improve the overall system performance by modifying the online isotope calibration procedure to reduce nonlinearity problems and reconfiguring the manifold plumbing to eliminate inlet bias due to pressure transient. The problems of nonlinearity and inlet bias were two major factors that limited the system performance (Lee et al., 2005). They must be dealt in the application of the micrometeorological flux-gradient method to measure the flux isotope ratio of evapotranspiration, where it is crucial to attain high precision of the water vapor D/H and $^{18}O/^{16}O$ isotope ratios (Lee et al., 2007). The lessons learned here may also be useful for other in situ measurement systems.

Our third objective was to refine a method that can be used to provide independent, timely performance test of the in situ system in field conditions. The method, briefly described in Lee et al. (2005), used a dewpoint generator to generate a moist air stream whose D/H and $^{18}O/^{16}O$ isotope ratios follow the Rayleigh distillation prediction.

To date, the majority of water vapor isotope studies have relied on the cold-trap/mass spectrometry methods (Yakir and Wang, 1996; Yakir and Sternberg, 2000; Tsujimura et al., 2007). However, the cold-trap methods are not ideally suited for the purpose of verification of the in situ observation, for three reasons. First, they require significant amount of manual, time consuming operation. Second,

they are prone to measurement errors caused by incomplete trapping efficiencies (Schoch-Fischer et al., 1983). Finally and most importantly, the result is not known until the trapped vapor sample is analyzed by a mass spectrometer, usually housed in a laboratory far away from the field. Such delay makes timely detection of system malfunction very difficult.

Materials and methods

TDL analyzer, sampling and calibration system

The TDL (tunable diode laser) analyzer used in this study was an upgraded version from the one described by Lee et al. (2005). It used absorption lines for HDO, $H_2{}^{18}O$ and $H_2{}^{16}O$ at wavenumbers of 1501.116, 1501.188 and 1500.546 cm^{-1}, respectively. The analyzer scanned these absorption lines in a rapid alternating fashion, providing nearly simultaneous detection of the molar fractions of the three isotopes. The laser's emission wavenumber depended on its temperature and current. As the temperature of the laser changed, its bias current was automatically adjusted to maintain the correct emission frequency. The laser's optical power output depended on the bias current, leading to measurement errors due to detector non-linearity. Ideally, each absorption line should have identical effective strength, thereby reducing errors related to the non-linear response of the sample and reference detectors. In reality, this was difficult to achieve. In the present study, the reference cell absorption was 94.3%, 85.8% and 86.5% for $H_2{}^{16}O$, HDO and $H_2{}^{18}O$, respectively, at the absorption line center, when zero air was supplied to the sample cell. The reader is reminded that the reference detector sees both the reference cell and the sample cell through a beam splitting arrangement (Edwards et al., 2003).

A schematic diagram of the analyzer, sampling and calibration system was shown in Fig. 1. The analyzer was configured with a six-intake manifold, with three air sample intakes and three calibration gas intakes including two calibration streams generated by an in situ calibration device (S1 and S2; see Section 'Calibration procedure'). Flow through the calibration intakes were controlled at about 0.3 L min^{-1} by stainless steel precision needle valves and flow in the air intakes was controlled at 0.6–2 L min^{-1} by stainless steel critical orifices. The pressure upstream of the manifold was typically less than 300 hPa, minimizing vapor condensation within the delivery tubing. A subsample (0.2 L min^{-1} STP) was drawn from one of the six intakes into the analyzer's sample cell. The subsampling arrangement effectively removed the pressure transient during manifold switching, a significant improvement over the system described by Lee et al. (2005). In the following tests, two of the air intakes were blocked. The switching sequence was S1, S2, air, and zero, with 25 s spent on each intake.

The analyzer's reference cell was supplied with pure water vapor drawn from a reference water reservoir, composed of 5 g D_2O, 1 g $H_2{}^{18}O$ and 100 g $H_2{}^{16}O$. The highly enriched composition of the reference water resulted in roughly the same level of absorption for all three isotopologues considered here. The airflows through the reference and sample cells were drawn to the sample pump. The sample and reference cells operated at a low pressure (typically <10 hPa), reducing the absorption line width to minimize absorption from interfering species. The low operating pressure also increased the turnover of the air in the sample cell because volume flow rate was inversely proportional to pressure, thus reducing the instrument time constant.

Nonlinearity correction

One of the major challenges in measuring the vapor isotope ratio lies in instrument nonlinearity. Non-linear errors in the measurement of HDO, $H_2{}^{18}O$ and $H_2{}^{16}O$ could arise from non-linear response in the reference and sample detectors or from the multi-mode output (i.e. emission at undesired frequencies) from the laser. The absorption lines are not strong enough to give a definitive measurement of the laser multimode power, but it was clearly less than 2%. The correction method for nonlinearity is outlined below.

In the TDL software the nonlinearity problem was expressed as

$$w = w_1 + rw_1^2, \quad (1)$$

where w is the linearized sample detector response, w_1 is the raw sample detector response, and r is a nonlinearity coefficient. This correction was applied on each point of the measured transmittance spectrum before it was used to calculate the concentration. The nonlinearity coefficient was tuned using a dew point generator (LI610, Licor Inc., Lincoln, NE, USA) to provide a sample air stream with dewpoint of 1, 5, 10, 15, or 20 °C. An optimal value was chosen for r so that the TDL measurement of H_2O matched the dewpoint generator mixing ratio.

Next, we used the two calibration streams (S1 and S2) with identical isotope ratio but roughly 10% different water mixing ratios, to further optimize the nonlinearity parameter. After all optical parameters of the laser had been tuned, we ran a series of tests with the dripper set to a constant dripping rating. We then used S2 as a standard to calibrate the reading of S1 (see Eq. (3) below). If the analyzer was perfectly linear, the calibrated S1 isotope ratio should be identical to the S2 value. Otherwise, the nonlinearity parameter was not optimized and was adjusted accordingly. The process was repeated until a suitable value of the nonlinearity parameter was found so that the calibrated S1 reading was within 0.5 per mil (^{18}O) of the S2 standard over the range of mixing ratio expected for the experimental period.

Calibration procedure

A dripping system (henceforth referred to as dripper), consisting of a syringe pump and an evaporating flask (labeled as mixing volume in Fig. 1), was used to generate two calibration standard gases (S1 and S2). The syringe pump delivered liquid water of known isotope ratio ($-104.0‰$ for D/H, and $-14.13‰$ for $^{18}O/^{16}O$) at a rate of 1–12 μL min^{-1} into the flask which was also fed with dry air. The dry air flow was controlled and updated every 10 min so that the moist air out of the flask had a water vapor mixing ratio (S2) that was about 5% high than the ambient water vapor mixing ratio. A portion of the moist air was mixed with a small amount of dry air to produce the second calibration stream

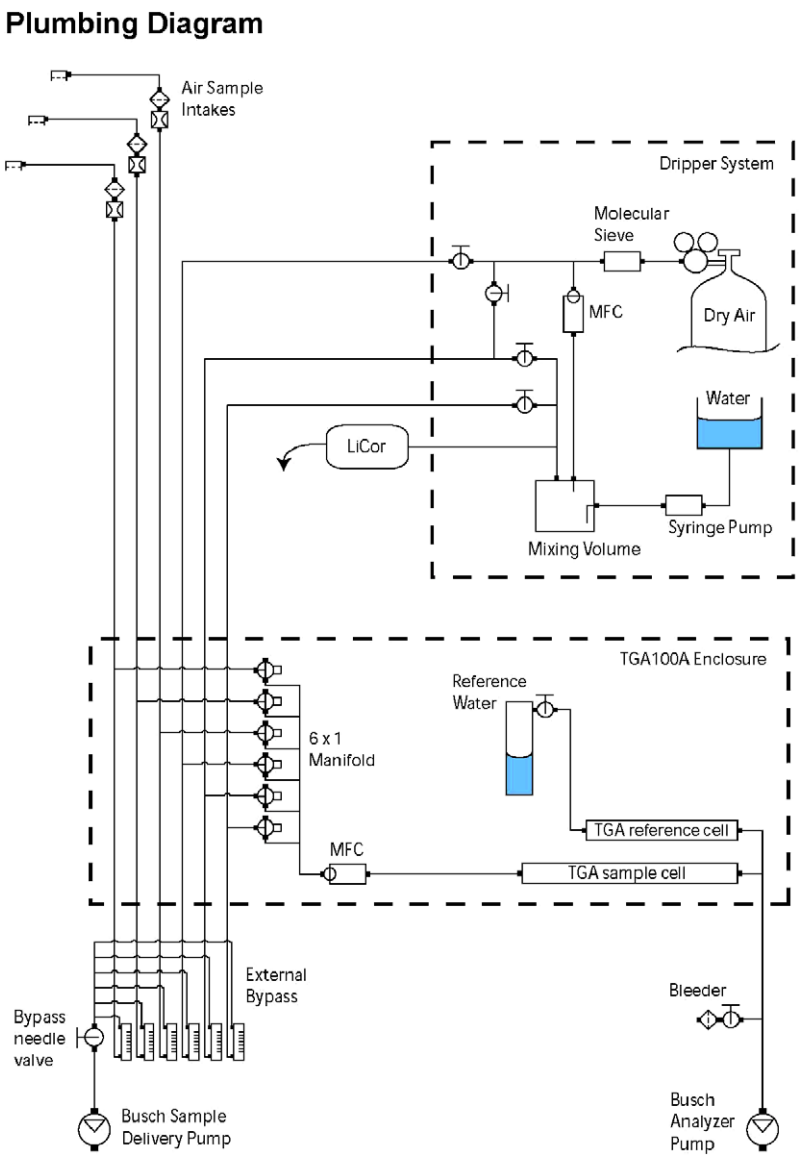

Figure 1 Schematic diagram of the TDL analyzer, sampling and calibration system for water vapor D/H and $^{18}O/^{16}O$ isotopes. The manifold consists of six small solenoid valves (72 μL internal volume, model LHDA1223211H, The Lee Company, Westbrook, Connecticut).

(S1) whose mixing ratio was about 5% lower than the ambient mixing ratio. Because evaporation occurred instantly in the evaporating flask, the two calibration streams had isotope ratios that were identical to the liquid water feed ($-104.0‰$ for D/H and $-14.13‰$ for $^{18}O/^{16}O$). Zero calibration was accomplished with a tank of commercial dry grade air fit with a molecular sieve.

The calibration of the ambient vapor measurement was accomplished in two steps. First, let x_i be the TDL uncalibrated volume $H_2{}^{16}O$ mixing ratio for intake i ($i = 1, 2, 3, 4$ for S1, S2, zero and air, respectively), and x'_i be the uncalibrated volume mixing ratio of the minor species (HDO or $H_2{}^{18}O$). The vapor molar ratio (D/H or $^{18}O/^{16}O$) was given by

$$R_1 = R_d \frac{x'_4 - x'_3}{x'_1 - x'_3} \frac{x_1 - x_3}{x_4 - x_3}, \quad (2)$$

if S1 was used as the calibration gas, or

$$R_2 = R_d \frac{x'_4 - x'_3}{x'_2 - x'_3} \frac{x_2 - x_3}{x_4 - x_3}, \quad (3)$$

if S2 was used for calibration, where R_d is molar ratio of the dripper water feed. The correction factor $(x_1 - x_3)/(x'_1 - x'_3)$ was found to vary by 7% peak-to-peak for HDO and 2% for $H_2{}^{18}O$. The molar mixing ratio was converted to the delta notation as

$$\delta_1 = (R_1/R_{vsmow} - 1) \times 1000‰, \quad (4)$$

and

$$\delta_2 = (R_2/R_{vsmow} - 1) \times 1000‰, \quad (5)$$

Next, to further reduce the analyzer nonlinearity error, we used a linear interpolation between δ_1 and δ_2 to find the true ambient isotope ratio

$$\delta_v = \delta_1 + \frac{(\delta_2 - \delta_1)}{(x_2 - x_1)}(x_4 - x_1). \quad (6)$$

The system nonlinearity was checked weekly to ensure that the difference between δ_1 and δ_2 was within the tolerable threshold of 0.5‰ (^{18}O). So the correction term (second term on the right of Eq. (6)) could be as large as 0.5‰. For reasons that we do not yet understand, nonlinearity was much less of a problem for HDO.

In mass spectrometer analysis, it is desirable to use multiple isotope standards to correct for the stretching of the delta scale. This was not done here. Instead, our real-time calibration procedure was made at a single isotope ratio and optimized to handle the dynamic and concurrent changes in the absolute abundance (volume mixing ratio) of the individual isotopologues. This is because the analyzer described here was a fundamentally different instrument from a mass spectrometer. The latter requires only a tiny amount of water sample, allowing for a measurement scheme in which the isotopologue signals are always at approximately the same level. In real-time atmospheric measurements, the dynamic change in the mixing ratios is much larger than the stretching of the delta scale. For example, over the course of a few days in November 2006, the mixing ratios varied by a factor of 5 whereas the change in the isotope ratio was less than 200‰ for D/H and 30‰ for $^{18}O/^{16}O$, corresponding to only 20% and 3% deviation, respectively, from the calibration stream mixing ratios (see Section 'Results of the atmospheric measurement').

Laboratory tests

Tests with a dewpoint generator

The commercially available dewpoint generator (LI610, Licor Inc., Lincoln, NE, USA) was a useful tool for the TDL performance evaluation. It served two functions. First, the moist air from the generator, because it followed the Rayleigh prediction, was used to assess the accuracy and precision of the TDL measurement. Second, with the appropriate combination of initial water mass and flow rate, the isotope contents of the moist air varied over a sufficient range, allowing an assessment of the possibility of isotope stretching mentioned above. Here, we did dewpoint tests at dewpoint settings of 15, 12, 8, and 1 °C with 2–3 tests at each dewpoint temperature. Each dewpoint test was run for 24 h, following the procedure described below:

(a) *Test preparation*: Water in the dewpoint generator reservoir was withdrawn and discarded. The reservoir was then flushed several times with 20 mL of the calibration water whose isotope ratio was identical to that of the dripper water. The reservoir was again emptied. Next, it was filled with 30–35 mL of the calibration water. In the final preparation step, the dewpoint generator was cooled to the set dewpoint temperature for 3–4 h to allow air in the dewpoint internal plumbing to reach full equilibrium with the calibration water.

(b) *Test*: The dewpoint generator was fed with dry air. Its flow was turned on to a rate of 700 mL min^{-1} with the start time noted. Of this flow, 570 mL min^{-1} was delivered to the TDL analyzer via its air intake and the remaining flow was bled to the room. The test was run for 24 h.

(c) *End of the test*: The dewpoint generator was turned off, with the ending time noted. The water remaining in the reservoir was withdrawn completely with a syringe and its weight was measured. A small portion (2 mL) was archived for later analysis of its isotope content by a mass spectrometer. The amount of water loss during the test depended on the dewpoint setting, typically varying from 4.8 g at 1 °C to 11.5 g at 15 °C over the 24 h period. Similarly, the amount of enrichment also depended on dewpoint temperature and varied from 12‰ (D/H) and 2‰ ($^{18}O/^{16}O$) at 1 °C to 23‰ and 3‰ at 15 °C. The mass flow of water vapor from the generator was given by

$$Q = (m_0 - m_e)/(t_e - t_0), \quad (7)$$

where m_0 and m_e are the initial and final mass of the reservoir water and t_0 and t_e are the start and end time of the test.

The molar isotope ratio of the water vapor generated by the dewpoint generator follows the familiar Rayleigh distillation equation

$$R_v = \frac{R_{l,0}}{\alpha}\left(\frac{m}{m_0}\right)^{1/\alpha - 1}, \quad (8)$$

where R_v is the water vapor isotope of D/H or $^{18}O/^{16}O$, and $R_{l,0}$ is the initial isotope ratio of the calibration water, and the residual water mass (m) in the reservoir is given by

$$m = m_0 - Qt. \quad (9)$$

The molar ratio was converted to the δ-notation. Since the air in the reservoir headspace was saturated, the fractionation factor α should equal the equilibrium fractionation factor, given for deuterium by

$$\alpha = \exp[24844/(t_d + 273)^2 - 76.248/(t_d + 273) + 52.612 \times 10^{-3}], \quad (10)$$

and for oxygen-18 by

$$\alpha = \exp[1137/(t_d + 273)^2 - 0.4156/(t_d + 273) - 2.0667 \times 10^{-3}] \quad (11)$$

(Majoube, 1971), where t_d (°C) is the temperature of the water reservoir of the dewpoint generator.

Atmospheric measurement

Our TDL system drew ambient air through one sample intake from the outside of our laboratory in Beijing, China (Fig. 1), and has been operated since the late November in 2006 except for the period of the dewpoint tests mentioned above. The intake inlet filter (Swagelok model B-4F-05, Connecticut Valves and Fittings, Norwalk, Connecticut) and the critical orifice were contained in an enclosure heated to 60 °C, minimizing the possibility of condensation. The TDL signals (uncalibrated mixing ratio) were recorded at 1 Hz by a datalogger (Model CR1000, Campbell Scientific Inc., Logan, UT, USA) and then block-averaged over 25 s intervals for analysis and archiving. The data reported in this study were block-averaged to hourly intervals.

A comparative study was done on day 325, 345, 355, 356 and 359 in 2006 between the TDL system and the traditional cold-trap/mass spectrometry method. Atmospheric water vapor was collected through glass traps immersed in an alcohol/liquid nitrogen solution, using a setup modified according to Helliker et al. (2002). The low temperature of the solution was maintained by periodically adding liquid nitrogen. Each collection lasted 60 min. The weight of the collected vapour sample was within 10% of that expected from the ambient mixing ratio, flow rate, air temperature, and pressure. All liquid samples, including the trapped vapor samples and dewpoint test samples, were analyzed for their isotope ratios by pyrolysis with a continuous flow method on a mass spectrometer (Finnigan Inc., MAT 253). The precision of the analysis (one standard deviation) was ±2‰ for D/H and ±0.3‰ for $^{18}O/^{16}O$.

Results and discussion

TDL measurement precision

Fig. 2 gives an example of Allan variance analysis of both the calibrated and uncalibrated isotope ratio time series. Table 1 summarizes the precision of the TDL measurement at four levels of dewpoint temperature. The results are given as one standard deviation of the difference between the measured isotope ratio and the value modeled according to the Rayleigh distillation equation. The precision improved as air became more moist or as averaging intervals increased. At the dewpoint temperature of 1 °C, the precision of the D/H and $^{18}O/^{16}O$ isotope ratios was 11.3‰ and 0.66‰ at 25 s intervals, respectively, and improved to 2.0‰ and 0.12‰, respectively, with hourly averaging. At the dewpoint temperature of 15 °C, the precision of the D/H and $^{18}O/^{16}O$ isotope ratio was 3.2‰ and 0.33‰, respectively, at 25 s intervals, and improved to 1.1‰ and 0.07‰ at hourly intervals, respectively. According to the Allan variance analysis, the precision of the D/H ratio continued to improve as the averaging interval increased beyond 1 h, indicative of a stable performance of the analyzer. The uncalibrated $^{18}O/^{16}O$ had the smallest standard deviation at an averaging interval of 400 s. After calibration, its precision improved with increasing averaging interval. In the following, the measurement was given at hourly intervals for convenience of presentation. As with $^{18}O/^{16}O$, our hourly D/H precision was comparable to the precision of mass spectrometry. In comparison, the 2-min precision of the TDL system is 0.25‰ for $^{13}CO_2/^{12}CO_2$ (Bowling et al., 2003) and 0.26‰ for $C^{18}O^{16}O/C^{16}O_2$ (Griffis et al., 2005). Lee et al. (2005) reported an hourly precision of 0.09 per mil for $^{18}O/^{16}O$ at a dewpoint temperature of 13 °C. The measurement precision in the present study was primarily limited by the spectral signal noise. Occasional dripper instability was also a limiting factor.

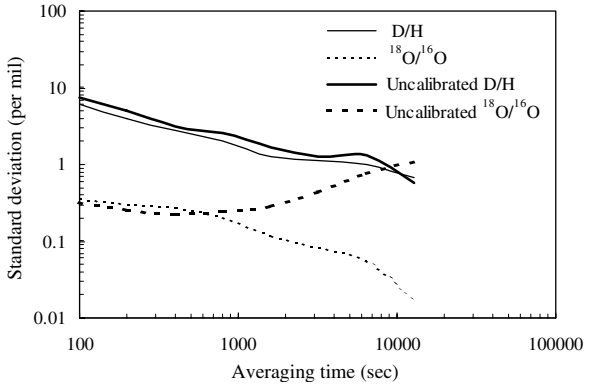

Figure 2 Allan variance analysis of the data collected during the dewpoint test as analyzed in Fig 4.

Table 1 Precision (‰) of the TDL measurement for D/H and $^{18}O/^{16}O$ at four levels of dewpoint temperature. Results are given as one standard deviation

t_d	w^{16}	D/H		$^{18}O/^{16}O$	
		25-s avg	1-h avg	25-s avg	1-h avg
15	15.9	3.2	1.1	0.33	0.07
12	13.0	4.9	1.1	0.33	0.08
8	9.7	6.0	1.5	0.43	0.07
1	5.6	11.3	2.0	0.66	0.12

Here, t_d is dewpoint temperature (°C), and w^{16} is the $H_2{}^{16}O$ mixing ratio (mmol mol^{-1}).

The precision of the TDL measurement was not obtained at lower water vapor mixing ratio because the dewpoint generator was not able to generate moist air with a dewpoint lower than the freezing point. To gain an appreciation of the precision at low humidity, we note that the ambient water vapor mixing ratios stayed almost constant at 1.5 mmol mol^{-1} (dewpoint temperature −18 °C) between 4:00 and 9:00 on January 8 in 2006. The 1-h average D/H isotope ratio had a value of −243.3 ± 5.7‰ and the 1-h average $^{18}O/^{16}O$ isotope ratio had a value of −36.73 ± 0.44‰. The actual instrument precision was likely to be better than the observed standard deviation as some of the variations in the vapor isotope ratios were caused by atmospheric processes.

Comparison with the Rayleigh distillation prediction

Comparisons of the TDL measurement of the water vapor generated by the dewpoint generator with that predicted from the Rayleigh distillation theory were done over the elapsed time at four levels of dewpoint temperature. Two typical examples of the measured and predicted time series were illuminated in Figs. 3 and 4. Fig. 3 represents the first dewpoint test we completed. The test started right after refill of the generator's reservoir with the calibration water. There was a downward trend in the measured D/H and $^{18}O/^{16}O$ ratios for about 3 h at the start of the test. This phenomenon was indicative that the airspace within the generator's internal plumbing did not reach full equilibrium with the reservoir water. In the subsequent tests, the dewpoint generator was cooled to the desired dewpoint temperature for at least 3 h. The agreement was noticeably improved (Fig. 4). In agreement with the Rayleigh distilla-

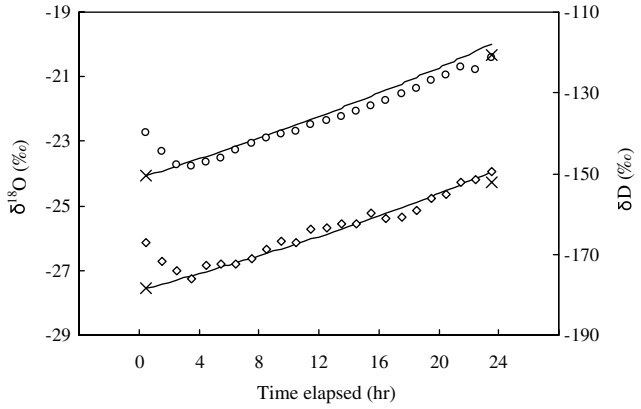

Figure 3 Comparison of the measured isotope ratio of water vapor (diamond for D/H, and circles for $^{18}O/^{16}O$) generated by a dewpoint generator at a temperature of 15 °C with that predicted from the Rayleigh distillation equation (solid line). Crosses indicate isotope ratio of water vapor in equilibrium with the liquid water in the generator.

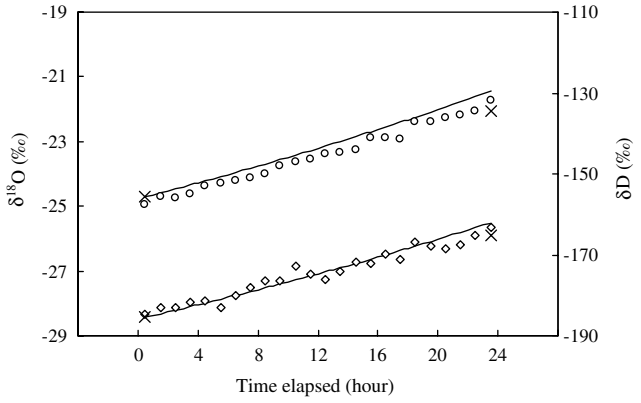

Figure 4 Same as Fig. 3 except for dewpoint temperature of 8 °C.

tion prediction, the measured isotope ratios of the water vapor from the dewpoint generator became progressively enriched with D and ^{18}O as time elapsed.

To further characterize the measurement accuracy, we did three additional analyses (Tables 2 and 3). In the first analysis, the first valid hourly TDL observation was compared with the Rayleigh equilibrium calculation. As in Lee et al. (2005), prior to the comparison, a small adjustment was made to the initial D/H and $^{18}O/^{16}O$ isotope ratios of the liquid water according to Eq. (8) to account for the change between the start of the dewpoint test and the first valid TDL measurement. In some cases where there was evidence that the dewpoint generator did not reach full equilibrium with its reservoir water, the first valid observation was chosen from the hour after the declining trend in the measurement was reversed (e.g. the fourth data point in Fig. 3). Excellent agreement existed between the measured and predicted D/H and $^{18}O/^{16}O$ isotope ratios at the beginning of the dewpoint test. The difference between the measured and predicted isotope ratios was $1.1 \pm 1.9‰$ for D/H (mean ± one standard deviation; Table 2) and $-0.06 \pm 0.13‰$ for $^{18}O/^{16}O$ (Table 3).

In the second analysis, the TDL observation was compared with the hourly equilibrium prediction according to Eq. (8) at the end of dewpoint test. The TDL observations, especially for $^{18}O/^{16}O$, became more negative with time than the Rayleigh distillation prediction. The difference for D/H and $^{18}O/^{16}O$ was $-1.2 \pm 1.4‰$ (Table 2) and $-0.39 \pm 0.13‰$ (Table 3), respectively, and was larger than the differences seen at the beginning of the test. Lee et al. (2005) attributed the larger difference to the contamination of the reservoir water by vapor in the room air.

In the third analysis, we removed the contamination effect by comparing the last hourly TDL observation with the equilibrium calculation according to Eq. (8) with the measured D/H and $^{18}O/^{16}O$ isotope values of the water sample withdrawn from the dewpoint reservoir after the test had ended. Instead of projecting forward in time, we used Eq. (8) to predict backward the isotope value for the last hour of valid TDL observation. This comparison yielded a bias of $0.7 \pm 2.0‰$ for the D/H isotope ratio (Table 2) and $0.15 \pm 0.22‰$ for the $^{18}O/^{16}O$ isotope ratio (Table 3). The bias of the third comparison decreased by $0.5‰$ for D/H and $0.24‰$ for $^{18}O/^{16}O$ relative to the second comparison, but the results were a little more variable. If the data from the first and third analysis were combined, the overall bias was $0.9 \pm 1.9‰$ for D/H and $0.04 \pm 0.20‰$ for $^{18}O/^{16}O$. These results were consistent with our precision characterization (Table 1). The $^{18}O/^{16}O$ results were improved over those reported by Lee et al. (2005) for the same type of tests ($-0.14 \pm 0.44‰$). We attribute the improvement to the modified calibration procedure and the new flow configuration that had eliminated the inlet bias associated with the pressure transient during valve switching (Fig. 1).

The two-point calibration procedure (Eq. (6)) was used in the above performance assessment. The performance would degrade if only one calibration stream was used: for this particular analyzer, a one-stream calibration could result in a systematic bias of up to 0.5 per mil in ^{18}O. In comparison, the D/H measurement was less sensitive to the nonlinearity error.

Fig. 5 shows the relationships between the D/H and $^{18}O/^{16}O$ isotope ratios based on the TDL measurement and the Rayleigh distillation prediction for the two dewpoint tests described in Figs. 3 and 4. The Rayleigh theory predicts the following relationship (Criss, 1999)

$$\delta_v D = (1000 + \delta D_i)\left(\frac{1000 + \delta_v^{18}O}{1000 + \delta_v^{18}O_i}\right)^{(1/\alpha_D - 1)/(1/\alpha_{18} - 1)} - 1000, \quad (12)$$

where $\delta_v D$ and $\delta_v{}^{18}O$ are the D/H and $^{18}O/^{16}O$ ratios of water vapor in the dewpoint generator, and δD_i and $\delta^{18}O_i$ are the initial D/H and $^{18}O/^{16}O$ ratios of water vapor, and α_D and α_{18} are equal the equilibrium fractionation factor for deuterium and oxygen-18, respectively (Eqs. (10) and (11)). The measured isotope values also followed Rayleigh relationship. A small but systematic bias from the Rayleigh line was evident. The primary reason was that contamination of the vapor in room air appeared to be more severe, in relative terms, for ^{18}O than for D. Indeed, the δD versus $\delta^{18}O$

Table 2 Results of the dewpoint test: δ, the TDL measurement of the water vapor D/H ratio (‰); δ_v, the vapor D/H ratio in equilibrium with the liquid water in the reservoir (‰); δ^*, the vapor D/H ratio of the forward prediction from the Rayleigh distillation theory (‰)

t_d	w^{16}	Start			End				
		δ	δ_v	$\delta - \delta_v$	δ	δ_v	δ^*	$\delta - \delta_v$	$\delta - \delta^*$
15	15.9	−175.9	−175.3	−0.6	−149.7	−152.1	−149.7	2.4	0.0
15	16.0	−172.3	−174.2	2.0	−151.3	−149.7	−149.3	−1.6	−2.1
15	15.9	−174.6	−175.4	0.8	−154.0	−150.4	−150.2	−3.6	−3.8
12	13.0	−180.7	−180.5	−0.2	−158.3	−159.8	−156.7	1.5	−1.6
12	12.9	−182.0	−180.6	−1.4	−157.2	−158.3	−157.6	1.1	0.4
8	9.8	−181.3	−185.4	4.2	−159.5	−162.4	−159.6	2.9	0.1
8	9.6	−184.6	−185.5	0.9	−163.1	−165.3	−162.1	2.2	−1.0
1	5.6	−188.2	−191.4	3.2	−178.4	−179.4	−178.3	1.0	−0.1
1	5.6	−193.9	−193.1	−0.8	−178.6	−180.0	−175.8	1.4	−2.8
1	5.6	−188.8	−192.0	3.1	−178.7	−178.9	−177.8	0.1	−1.0
Mean ± 1 std. dev.				1.1 ± 1.9				0.7 ± 2.0	−1.2 ± 1.4

Here, t_d is dewpoint temperature (°C), and w^{16} is the $H_2{}^{16}O$ mixing ratio (mmol mol^{-1}).

Table 3 Same as Table 2 except for $^{18}O/^{16}O$

t_d	w^{16}	Start			End				
		δ	δ_v	$\delta - \delta_v$	δ	δ_v	δ^*	$\delta - \delta_v$	$\delta - \delta^*$
15	15.9	−23.76	−23.62	−0.14	−20.41	−20.31	−19.98	−0.10	−0.43
15	16.0	−23.51	−23.46	−0.05	−20.36	−20.23	−19.93	−0.13	−0.43
15	15.9	−23.47	−23.63	0.16	−20.29	−20.36	−20.06	0.07	−0.23
12	13.0	−24.21	−24.21	0.00	−21.29	−21.72	−20.86	0.43	−0.43
12	12.9	−24.19	−24.22	0.03	−21.54	−21.52	−20.98	−0.02	−0.56
8	9.8	−24.73	−24.71	−0.02	−21.71	−21.88	−21.11	0.17	−0.60
8	9.6	−24.94	−24.72	−0.22	−21.71	−22.04	−21.45	0.33	−0.26
1	5.6	−25.36	−25.18	−0.18	−23.66	−23.92	−23.37	0.26	−0.29
1	5.6	−25.64	−25.42	−0.22	−23.41	−23.89	−23.04	0.48	−0.37
1	5.6	−25.23	−25.25	0.02	−23.58	−23.58	−23.30	−0.00	−0.28
Mean ± 1 std. dev.				−0.06 ± 0.13				0.15 ± 0.22	−0.39 ± 0.13

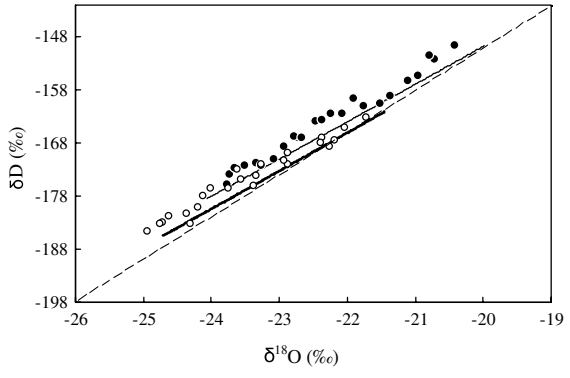

Figure 5 Plot of the measured water vapor D/H versus $^{18}O/^{16}O$ isotope ratio for dewpoint temperature of 8 °C (circles) and 15 °C (dots) with that predicted from the Rayleigh distillation equation (thick solid line for 8 °C and thin solid line for 15 °C). For comparison, the GMWL line ($\delta D = 8\delta^{18}O + 10$) is shown as a dashed line.

plot provides better diagnostic information on the contamination problem than the time series plot (Figs. 3 and 4).

Results of the atmospheric measurement

Table 4 summarizes the results of the TDL measurement of the D/H and $^{18}O/^{16}O$ isotope ratios and the cold trap/mass spectrometer analysis of water vapor samples. A total of 21 water vapor samples were collected on day 325, 345, 355, 356 and 359 in 2006, spanning a range of $H_2{}^{16}O$ mixing ratio of 2.4—6.9 mmol mol^{-1}. For the comparison, the TDL measurement was averaged to hourly intervals that matched the cold trap collection time. The difference between the TDL measurement and the cold-trap method was 1.2 ± 6.0‰ (mean ± one standard deviation) for D/H and 1.08 ± 1.30‰ for $^{18}O/^{16}O$ (Table 4). The standard deviation was larger than that of the dewpoint tests and was attributed to the difficulties in condensing out all the water vapor in the air stream and errors of the mass spectrometer and TDL system. The linear regression indicated relatively good agreement for both D/H ($y = 1.01x$, $R^2 = 0.98$, $n = 21$,

Table 4 Comparison of the D/H and $^{18}O/^{16}O$ isotope ratio of the ambient water vapor by the TDL measurement (δ, ‰) and the mass spectrometry analysis of water vapor samples collected with cold traps (δ_{trap}, ‰)

Day	Time (LST)	w^{16}	D/H			$^{18}O/^{16}O$		
			δ	δ_{trap}	$\delta - \delta_{trap}$	δ	δ_{trap}	$\delta - \delta_{trap}$
325	1020–1120	5.6	−136.2	−134.9	−1.3	−18.12	−18.56	0.44
	1123–1223	6.0	−129.6	−132.2	2.7	−17.13	−17.55	0.41
	1227–1327	6.4	−126.7	−129.0	2.4	−16.25	−17.48	1.23
	1329–1429	5.7	−137.1	−138.4	1.3	−17.96	−18.22	0.27
	1535–1635	5.5	−142.8	−140.8	−2.1	−18.17	−17.64	−0.53
	1638–1738	5.5	−140.1	−129.8	−10.4	−18.18	−17.47	−0.71
345	1000–1100	3.0	−197.1	−190.7	−6.4	−25.40	−27.98	2.58
	1300–1400	3.4	−157.7	−178.1	5.0	−23.83	−24.17	0.59
	1600–1700	3. 6	−170.1	−171.3	1.2	−22.59	−22.66	0.07
355	9000–1000	2.2	−220.0	−219.3	−0.7	−27.76	−28.62	0.86
	1100–1200	2.5	−215.8	−213.9	−1.9	−26.83	−26.98	0.15
	1300–1400	2.7	−198.9	−204.2	5.3	−25.16	−26.05	0.88
	1500–1600	2.9	−191.7	−194.9	3.2	−22.96	−24.53	1.57
	1700–1800	2.9	−194.9	−199.6	4.7	−24.90	−29.76	4.86
356	1100–1200	1.9	−255.0	−254.4	−0.6	−31.90	−32.90	0.99
	1300–1400	1.9	−252.3	−255.6	3.4	−31.94	−33.86	1.92
	1700–1800	1.8	−241.1	−250.8	9.7	−30.69	−32.63	1.95
	1900–2000	2.2	−219.1	−234.8	15.7	−28.81	−28.40	−0.41
359	1100–1200	3.4	−166.7	−156.2	−10.5	−20.53	−23.40	2.86
	1300–1400	3.5	−152.4	−150.6	−1.8	−19.37	−20.18	0.81
	1500–1600	3.6	−141.1	−146.7	5.6	−19.01	−20.93	1.92
Mean ± 1 std. dev.					1.2 ± 6.0			1.08 ± 1.30

Here, w^{16} is the $H_2{}^{16}O$ mixing ratio (mmol mol^{-1}).

where x is the TDL measurement and y is the cold traps/mass spectrometer analysis) and $^{18}O/^{16}O$ ($y = 1.05x$, $R^2 = 0.95$, $n = 21$). Lee et al. (2005) also found good agreement between the TDL and mass spectrometer measurements of $^{18}O/^{16}O$ in water vapor. Their TDL measurements differed from the cold-trap/mass spectrometer technique by −1.77‰ with a standard deviation of 1.75‰, or −0.36‰ with a standard deviation of 1.43‰ after correction to account for the vapor lost during the cold trap collection. The difference between the TDL and the cold trap data was more scattered than the laboratory data (Tables 2 and 3), suggesting a degraded TDL precision in real atmospheric measurements, problems in handling the cold-trap samples, or both.

Figs. 6a and b show the time series of all valid hourly D/H and $^{18}O/^{16}O$ isotope ratios measured with the TDL system in Beijing from day 322 to day 365 in 2006. For comparison, also shown are the isotope values of the water vapor samples collected with the cold trap method. Over this period, there was considerable variability in the isotope ratios of D/H and $^{18}O/^{16}O$. The changes in D/H and $^{18}O/^{16}O$ were highly correlated with that of the $H_2{}^{16}O$ mixing ratio, especially for the two sharp decreasing trends on day 349 and 361, times of cold front passage. The maximum values of D/H and $^{18}O/^{16}O$ were −117.6 and −14.78‰, respectively, and the minimum values were −370.3 and −51.72‰, respectively, during the experimental period. Even though the experimental period was rather short, considerable variations occurred, sometimes exceeding 200‰ for D/H and 25‰ for $^{18}O/^{16}O$ over just a few days. It would be difficult to capture such rapid variations with the cold trap method.

Fig. 7 shows the relationship between the D/H and $^{18}O/^{16}O$ isotope ratios from both the TDL and the cold trap methods. The GMWL line is also plotted for comparison. Most of the measured vapor values followed the GMWL line closely. However, a small group of data had D/H that was consistently higher than the GMWL line. These ''outliers'' came from the two periods with a sharp, decreasing humidity trend, as shown in Figs. 6a and b. They were beyond the humidity range over which the TDL was tested against the dewpoint generator, so the validity of the data might be called into question. However, tests over a much wider humidity range in our previous study does not reveal measurement artifacts at a low humidity except that the measurement precision degrades as humidity decreases (Lee et al., 2005). In these transitional periods, deuterium excess appeared to be distinctly different. A detailed examination of deuterium excess at various timescales such as season, weather cycle, rain event and diurnal variation is beyond the scope of this paper and will be investigated in our future work.

Conclusions

In this study, we have demonstrated the feasibility to simultaneously measure both D/H and $^{18}O/^{16}O$ in atmospheric water vapor using a commercially available tunable diode

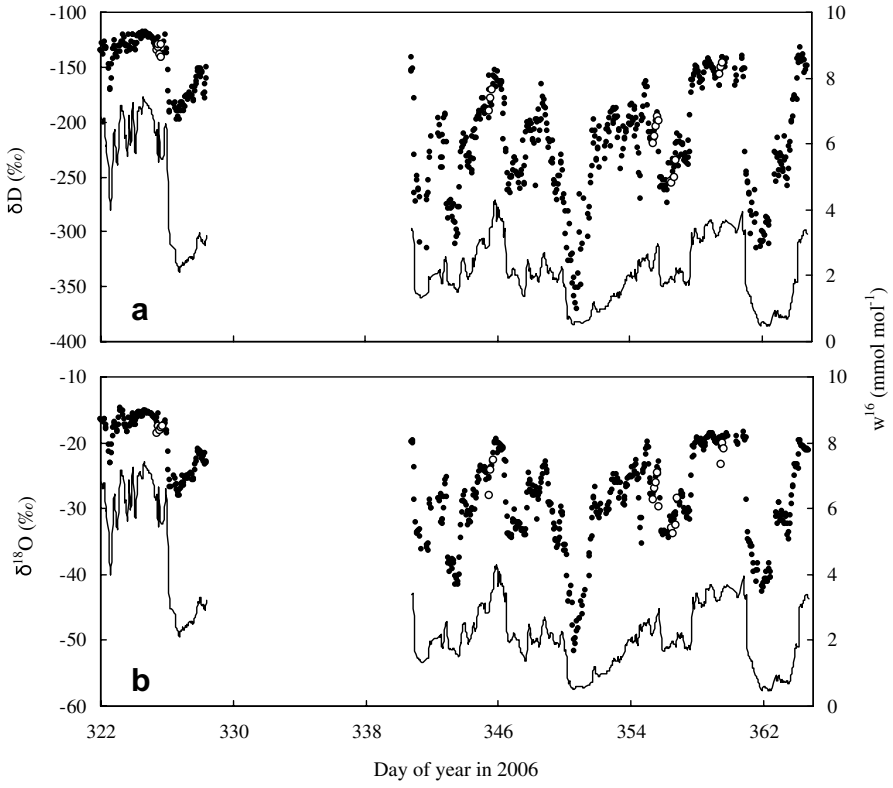

Figure 6 Time series of hourly average water vapor D/H (a) and $^{18}O/^{16}O$ (b) isotope ratio measured with the TDL system (dots), the cold traps/mass spectrometry approach (circles), and the $H_2{}^{16}O$ mixing ratio (solid line).

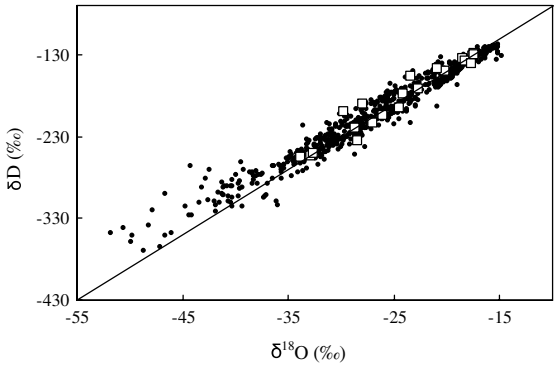

Figure 7 Relationship between the measured D/H and $^{18}O/^{16}O$ isotope ratios of ambient water vapor (dots: TDL; squares: cold trap). For comparison, the GMWL line is shown (solid line).

laser absorption spectrometer. Our atmospheric measurement agreed reasonable well with the cold trap method. It captured the rapidly changing isotopic signals in both D/H and $^{18}O/^{16}O$. The measured isotope ratios were highly correlated with the water vapor mixing ratio as expected (Lee et al., 2006) and followed very closely the GMWL line except during two transitional periods when the deuterium excess of atmospheric vapor appeared to deviate from the standard value.

The system described here was an improved version of that reported by Lee et al. (2005). In addition to the simultaneous detection of both D/H and $^{18}O/^{16}O$, improvement was made to the calibration procedure to reduce the nonlinearity problem and to the flow plumbing to remove manifold inlet bias. Our laboratory tests showed that the 1-h precision (one standard deviation) was 1.1‰ for D/H and 0.07‰ for $^{18}O/^{16}O$ at dewpoint temperature 15 °C.

We have refined a method to provide independent, timely performance test of the in situ system. The method used a dewpoint generator to generate a stream of moist air whose isotope ratio follows the Rayleigh distillation prediction. We showed that it can be used to characterize the precision of the TDL system. The procedure established here can be used to check the performance of other types of in situ measurement system in field conditions (e.g., Kerstel et al., 1999; Kuang et al., 2003; Gupta et al., 2005; Griffith et al., 2006).

Acknowledgements

This study was supported by the Chinese Academy of Sciences International Partnership Project ''Human Activities and Ecosystem Changes'' (Grant No. CXTD-Z2005-1), the National Natural Science Foundation of China (Grant No. 30670384), the Postdoctoral Science Foundation of China (Grant No. 20060390513), the Chinese National Science Foundation (Grant No. 30770409), and the US National Science Foundation Grant EAR-0229343. The first author also acknowledges the support through a START (Global Change System for Analysis, Research and Training) fellowship. We thank the two journal reviewers for their careful review of this paper.

References

Araguás-Araguás, L., Froehlich, K., Rozanski, K., 2000. Deuterium and oxygen-18 isotope composition of precipitation and atmospheric moisture. Hydrol. Process 14, 1341–1355.

Armengaud, A., Koster, RD., Jouzel, J., Ciais, P., 1998. Deuterium excess in Greenland snow: analysis with simple and complex models. J. Geophys. Res. 103, 8947–8953.

Bowling, D.R., Sargent, S.D., Tanner, B.D., Ehleringer, J.R., 2003. Tunable diode laser absorption spectroscopy for stable isotope studies of ecosystem–atmosphere CO_2 exchange. Agric. For. Meteorol. 118, 1–19.

Brunel, J.P., Simpson, H.J., Herczeg, A.L., Whitehead, R., Walker, G.R., 1992. Stable isotope composition of water vapor as an indicator of transpiration fluxes from rice crops. Water Resour. Res. 28, 1407–1416.

Cappa, C.D., Hendricks, M.B., DePaolo, D.J., Cohen, R.C., 2003. Isotopic fractionation of water during evaporation. J. Geophys. Res. 108, 4525–4534.

Ciais, P., White, J.W.C., Jouzel, J., Petit, J.R., 1995. The origin of present day antarctic precipitation from surface snow deuterium excess data. J. Geophys. Res. 100, 18917–18927.

Craig, H., 1961. Isotopic variations in meteoric waters. Science 133, 1702–1703.

Craig, H., Gordon, L.I., 1965. Deuterium and oxygen-18 variations in the ocean and the marine atmosphere. In: Tongiorgi, E. (Ed.), Proceedings of a Conference on Stable Isotopes in Oceanographic Studies and Paleotemperatures, Spoleto, Italy, pp. 9–130.

Criss, R.E., 1999. Principles of Stable Isotope Distribution. Oxford University Press, New York, 254p.

Dansgaard, W., 1964. Stable isotopes in precipitation. Tellus 16, 436–468.

Dawson, T.E., Pausch, R.C., Parker, H.M., 1998. The role of hydrogen and oxygen stable isotopes in understanding water movement along the soil–plant–atmospheric continuum. In: Griffiths, H. (Ed.), Stable Isotopes: Integration of Biological, Ecological and Geochemical Processes. Bios Scientific Publisher, Oxford, pp. 169–183.

Edwards, G.C., Thurtell, G.W., Kidd, G.E., Dias, G.M., Wagner-Riddle, C., 2003. A diode laser based gas monitor suitable for measurement of trace gas exchange using micrometeorological techniques. Agric. For. Meteorol. 28, 71–89.

Franz, P., Rochmann, T., 2005. High-precision isotope measurement of H_2O–O^{16}, H_2O–O^{17}, H2O–o18 and the delta O17 anomaly of water vapor in the southern lowermost stratosphere. Atmos. Chem. Phys. 5, 2949–2959.

Gat, J.R., 1980. The isotopes of hydrogen and oxygen in precipitation. In: Fritz, P., Fontes, J.Ch. (Eds.), Handbook of Environmental Isotope Geochemistry, vol. 1. Elsevier, pp. 21–47.

Gat, J.R., 1996. Oxygen and hydrogen isotopes in the hydrologic cycle. Annu. Rev. Earth Planet. Sci. 24, 225–262.

Gat, J.R., Klein, B., Kushnir, Y., Roether, W., Wernli, H., Yam, H., Shemesh, A., 2003. Isotope composition of air moisture over the Mediterranean sea: an index of the air–sea interaction pattern. Tellus 55B, 953–965.

Griffis, T.J., Baker, J.M., Sargent, S.D., Tanner, B.D., Zhang, J., 2004. Measuring field-scale isotopic CO_2 fluxes with tunable diode laser absorption spectroscopy and micrometeorological techniques. Agric. For. Meteorol. 124, 15–29.

Griffis, T.J., Lee, X., Baker, J.M., Sargent, S.D., King, J.Y., 2005. Feasibility of quantifying ecosystem–atmosphere C^{18} $O^{16}O$ exchange using laser spectroscopy and the flux-gradient method. Agric. For. Meteorol. 135, 44–60.

Griffith, D.W.T., Jamie, I., Esler, M., Wilson, S.R., Parkes, S.D., Waring, C., Bryant, G.W., 2006. Real-time field measurements of stable isotopes in water and CO_2 by Fourier transform infrared spectrometry. Isotope Environ. Health Stud. 42, 9–20.

Gupta, M., Owano, T., Baer, D., Provencal, R., Ricci, K., O'Keefe, A., Kendall, C., Doctor, D., Rollog, M., Silva, S., McDonnell, J., 2005. Development and validation of a field-deployable optical spectrometer for real-time, natural abundance measurements of O and H isotopes of water. Eos Trans. AGU 86 (52), Fall Meet. Suppl., Abstract H41C-0423.

He, H., Smith, R.B., 1999. Stable isotope composition of water vapour in the atmospheric boundary layer above the forests of New England. J. Geophys. Res. 104, 11657–11673.

Helliker, B.R., Roden, J.S., Cook, C., Ehleringer, J.R., 2002. A rapid and precise method for sampling and determining the oxygen isotope ratio of atmospheric water vapor. Rapid Commun. Mass Spectrom. 16, 929–932.

Horita, J., Wesolowski, D., 1994. Liquid-vapor fractionation of oxygen and hydrogen isotopes of water from the freezing to the critical temperature. Geochim. Cosmochim. Acta 58, 3425–3437.

Jouzel, J., 1986. Isotopes in cloud physics: multiphase and multistage condensation processes. In: Fritz, P., Fontes, J.Ch. (Eds.), Handbook of Environmental Isotope Geochemistry, vol. 2. Elsevier, pp. 61–112.

Jouzel, J., Russell, G., Suozzo, R., Koster, R., White, J.W.C., Broecker, W.S., 1987. Simulations of the HDO and H_2 ^{18}O atmospheric cycles using the NASA/GISS general circulation model: the seasonal cycle for present day conditions. J. Geophys. Res. 92, 14739–14760.

Jouzel, J., Hoffmann, G., Koster, R.D., Masson, V., 2000. Water isotopes in precipitation: data/model comparison for present-day and past climates. Quat. Sci. Rev. 19, 363–379.

Kavanaugh, J.L., Cuffey, K.M., 2003. Space and time variation of δ^{18} O and δD in Antarctic precipitation revisited. Glob. Biogeochem. Cycle 17, 1017. doi:10.1029/2002GB00191.

Kerstel, E.R.T., Iannone, R.Q., Chenevier, M., Kassi, S., Jost, H.J., Romanini, D., 2006. A water isotope (H2, O17 and O18) spectrometer based on optical feedback cavity-enhanced absorption for in situ airborne applications. Appl. Phys. B Lasers Opt. 85, 397–406.

Kerstel, E.R.T., Trigt, R., Dam, N., Reuss, J., Meijer, H.A.J., 1999. Simultaneous determination of the^2 $H/^1H$,^{17} $O/^{16}O$, and $^{18}O/^{16}O$ isotope abundance ratios in water by means of laser spectrometry. Anal. Chem. 71, 5297–5303.

Kuang, Z., Toon, G.C., Wennberg, P.O., Yung, Y.L., 2003. Measured HDO/H_2 O ratios across the tropical tropopause. Geophys. Res. Lett. 30, 1372. doi:10.1029/2003GL01702.

Lai, C.T., Ehleringer, J.R., Tans, P.P., Wofsy, S.C., Urbanski, S.P., Hollinger, D.Y., 2004. Estimating photosynthetic ^{13}C discrimination in terrestrial CO_2 exchange from canopy to regional scales, Glob. Biogeochem. Cycle 18, GB1041. doi:10.1029/2003GB00214.

Lai, C.T., Ehleringer, J.R., Bond, B.J., Paw U, K.T., 2006. Contributions of evaporation, isotopic non-steady state transpiration and atmospheric mixing on the $\delta^{18}O$ of water vapour in Pacific Northwest coniferous forests. Plant Cell Environ. 29, 77–94.

Lee, X., Kim, K., Smith, R., 2007. Temporal variations of the isotopic signal of the whole-canopy transpiration in a temperate forest. Glob. Biogeochem. Cycle. 21, GB3013. doi:10.1029/2006GB002871.

Lee, X., Sargent, S., Smith, R., Tanner, B., 2005. In situ measurement of the water vapor $^{18}O/^{16}O$ isotope ratio for atmospheric and ecological applications. J. Atmos. Ocean. Technol. 22, 555–565.

Lee, X., Smith, R., Williams, J., 2006. Water vapour $^{18}O/^{16}O$ isotope ratio in surface air in New England, USA. Tellus 58B, 293–304.

Majoube, M., 1971. Fractionnement en oxygene-18 et en deuterium entre l'eau et sa vapeur. J. Chim. Phys. 68, 1423–1436.

Merlivat, L., 1978. Molecular diffusivities of H_2 ^{16}O, $HD^{16}O$, and H_2 ^{18}O in gases. J. Chem. Phys. 69, 2864–2871.

Merlivat, L., Jouzel, J., 1979. Global climatic interpretation of the deuterium-oxygen 18 relationship for precipitation. J. Geophys. Res. 84, 5029—5033.

Peng, H., Mayer, B., Harris, S., Roy Krouse, H., 2004. A 10-yr record of stable isotope ratios of hydrogen and oxygen in precipitation at Calgary, Alberta, Canada. Tellus 56B, 147—159.

Schoch-Fischer, H., Rozanski, K., Jacob, H., Sonntag, C., Jouzel, I., Östlund, G., Geyh, M.A., 1983. Hydrometeorological factors controlling the time variation of D,^{18}O and ^{3}H in atmospheric water vapour and precipitation in the northern westwind belt. In: Street-Perrott, A. et al. (Eds.), Isotope Hydrology. IAEA Publ., pp. 3—30 (SM-270/19).

Tsujimura, M., Sasaki, L., Yamanaka, T., Sugimoto, A., Li, S.G., Matsushima, D., Kotani, A., Saandar, M., 2007. Vertical distribution of stable isotopic composition in atmospheric water vapor and subsurface water in grassland and forest sites, eastern Mongolia. J. Hydrol. 333, 35—46.

Vimeux, F., Masson, V., Jouzel, J., Petit, J.R., Steig, E.J., Stievenard, M., Vaikmae, R., White, J.W.C., 2001. Holocene hydrological cycle changes in southern hemisphere documented in East Antarctic deuterium excess records. Clim. Dyn. 17, 503—513.

Webster, C.R., Heymsfield, A.J., 2003. Water isotope ratios D/H, ^{18}O/^{16}O,^{17}O/^{16}O in and out of clouds map dehydration pathways. Science 302, 1742—1745.

Worden, J., Noone, D., Bowman, K., 2007. Importance of rain evaporation and continental convection in the tropical water cycle. Nature 445, 528—532.

Yakir, D., Sternberg, S.L., 2000. The use of stable isotopes to study ecosystem gas exchange. Oecologia 123, 297—311.

Yakir, D., Wang, X.F., 1996. Fluxes of CO_2 and water between terrestrial vegetation and the atmosphere estimated from isotope measurement. Nature 380, 515—517.